| | |
|---|---|
| Title: | Influence of Fatigue Loading in Shear Failures of Reinforced Concrete Members without Transverse Reinforcement |
| Authors: | Fernández Ruiz M., Zanuy C., Natário F., Gallego J.M., Albajar L., Muttoni A. |
| Published in: | Journal of Advanced Concrete Technology |
| DOI | 10.3151/jact.13.263 |
| Volume:<br>Pages: | vol. 13<br>pp. 263-274 |
| Country: | Japan |
| Year of publication: | 2015 |
| Type of publication: | Peer reviewed journal article |

| | |
|---|---|
| Please quote as: | Fernández Ruiz M., Zanuy C., Natário F., Gallego J.M., Albajar L., Muttoni A., *Influence of Fatigue Loading in Shear Failures of Reinforced Concrete Members without Transverse Reinforcement*, Journal of Advanced Concrete Technology, vol. 13, Japan, 2015, pp. 263-274. |

# Influence of fatigue loading in shear failures of reinforced concrete members without transverse reinforcement

Miguel Fernández Ruiz, Carlos Zanuy, Francisco Natário, Juan Manuel Gallego, Luis Albajar, Aurelio Muttoni

*Journal of Advanced Concrete Technology,* volume 13 (2015), pp. 263-274

*Scientific paper*

# Influence of Fatigue Loading in Shear Failures of Reinforced Concrete Members without Transverse Reinforcement

Miguel Fernández Ruiz[1], Carlos Zanuy[2], Francisco Natário[3*], Juan Manuel Gallego[4], Luis Albajar[5] and Aurelio Muttoni[6]

Received 21 January 2015, accepted 18 May 2015 doi:10.3151/jact.13.263

## Abstract

Shear fatigue of reinforced concrete members without transverse reinforcement has been observed to be potentially governing for the strength of some structural members subjected to large live loads of repetitive nature (as traffic, wind or wave actions). Although extensive experimental programmes have been performed in the past and a rational approach to the problem can be performed on the basis of Fracture Mechanics, most design codes still ground shear fatigue design on empirical equations fitted on the basis of existing data. These empirical formulas show inconsistency amongst them and some neglect potentially relevant parameters as the ratio of maximum and minimum fatigue load levels.

In this paper, a consistent design approach is presented, by using the principles of Fracture Mechanics applied to quasi-brittle materials in combination with the Critical Shear Crack Theory. This approach leads to a simple, yet sound and rational, design equation incorporating the different influences of fatigue actions (minimum and maximum load levels) and shear strength (size and strain effects, material and geometrical properties). The accuracy of the design expression is checked against available test data in terms of Wöhler (S-N) and Goodman diagrams, showing consistent agreement to experimental evidence. In addition, the estimate of the number of cycles until failure is shown to be significantly more accurate and with lower scatter than current empirical shear fatigue formulations of Eurocode 2 or *fib*-Model Code 2010.

## 1. Introduction

Fatigue problems in reinforced concrete elements have traditionally been associated to rupture of the reinforcing bars, normally due to bending actions. Nevertheless, investigations on the fatigue behaviour of some members such as bridge deck slabs (**Fig. 1a**) have shown that shear fatigue might be governing particularly for high values of the maximum applied shear force (Natário and Muttoni 2014; Gallego *et al*. 2014). Also, fatigue verifications may be governing for other structures exposed to large cyclic actions, such as wind towers and their foundations or offshore structures, refer to **Figs. 1b,c**. These cases related to structural engineering are usually governed by ratios of the minimum applied shear force to maximum applied shear force close to zero or can even be subjected to reversal actions.

In the past, most research on shear fatigue failures of reinforced concrete members has concentrated on beams tested under three- or four-point bending configuration. These experimental programmes have focused on analysing the influence of parameters like the shear span-to-depth ratio ($a/d$), the flexural reinforcement amount ($\rho = A_s/bd$), the concrete strength ($f_c$) or the influence of the maximum and minimum level of shear forces ($V_{max}$, $V_{min}$). One of the first most comprehensive and systematic testing was carried out by Chang and Kesler (1958a,b) in the fifties. They tested 64 beams under fatigue loading with a constant value of the shear slenderness ($a/d$ = 3.72) and three different flexural reinforcement amounts ($\rho$ = 0.0102, 0.0186 and 0.0289). According to their experimental results, Chang and Kesler

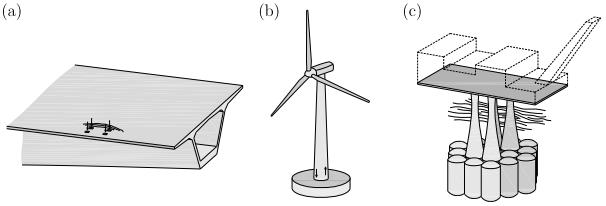


Fig. 1 Examples of structural elements potentially sensitive to shear fatigue failures: (a) bridge deck slabs; (b) wind towers; and (c) offshore platforms.

[1]Lecturer and Research Scientist, École Polytechnique Fédérale de Lausanne, ENAC, Lausanne, Switzerland.
[2]Assistant Professor, Universidad Politécnica de Madrid ETS Ingenieros de Caminos, Department of Continuum Mechanics and Structures, Madrid, Spain.
[3]PhD Candidate, École Polytechnique Fédérale de Lausanne, ENAC, Lausanne, Switzerland.
*Corresponding author,
*E-mail*: francisco.natario@epfl.ch.
[4]Postdoctoral Researcher, Swiss Federal Laboratories for Materials Science and Technology, Dübendorf, Switzerland.
[5]Professor, Universidad Politécnica de Madrid, ETS Ingenieros de Caminos, Department of Continuum Mechanics and Structures, Madrid, Spain.
[6]Professor, École Polytechnique Fédérale de Lausanne, ENAC, Lausanne, Switzerland.

identified two potential shear fatigue failure modes (refer to **Fig. 2**): shear-compression failure and diagonal cracking failure. Both were due to the development and propagation with the number of cycles of an eventually critical shear crack. In the former failure mode, the propagation of the crack limits the depth and strength of the compression zone near the load, which eventually crushes. In the latter, the critical shear crack propagates in an unstable manner leading to a sudden collapse of the member.

Stelson and Cernica (1958) tested 11 specimens with $\rho = 0.0290$ and similar cross section than those of Chang and Kesler, but higher shear slenderness ($a/d = 5.65$). Four specimens presented shear fatigue failures by diagonal cracking at a very similar number of load cycles to the corresponding series of Chang and Kesler. Verna and Stelson (1962) carried out 60 fatigue tests in reinforced concrete beams without stirrups. They focused on the description of fatigue failure and identified the following failure modes: shear fatigue, fatigue of the reinforcement, fatigue of concrete in compression and fatigue of the anchorage. The latter failure mode was related to the propagation of a diagonal crack towards the support and at the level of the longitudinal reinforcement, similar to the delamination cracks due to dowel action (Muttoni and Ruiz 2008). Taylor (1959) studied the influence of the type of reinforcement, by testing specimens with plain and ribbed bars with a constant value of the shear slenderness ($a/d = 4.1$) and for different amounts of flexural reinforcement. The results showed very similar fatigue strength of specimens with different reinforcement, even though the bond properties of reinforcement are known to play a significant role in the actions involved in resisting shear force (Muttoni and Ruiz 2008).

Shear fatigue tests carried out in Japan in late seventies focused on the influence of the shear slenderness and the load levels. Higai (1978) and Farghaly (1979) tested reinforced concrete beams with shear slenderness ranging from 1.5 to 6.4. Their results showed that the diagonal crack developed in the first cycle for the shortest specimens, but the residual fatigue life after diagonal cracking was much larger than specimens with higher shear slenderness. Moreover, a higher sensitivity to diagonal cracking failure than to shear-compression was observed as the shear slenderness increased. The influence of the ratio between the minimum and the maximum shear load ($R = V_{min}/V_{max}$) was investigated by Ueda (1982). His tests showed that elements subjected to higher values of parameter $R$ had higher fatigue life than elements tested with lower values of $R$.

Rombach and Kohl (2012, 2013) have recently tested 7 reinforced concrete beams with $a/d = 5.0$ and $\rho = 0.0157$, obtaining shear fatigue failure (by shear-compression) in the beams where the maximum load exceeded 60% of static strength. Other experimental works on lightly and normally reinforced beams ($\rho$ varying from 0.0052 to 0.016) (Schläfli and Brühwiller

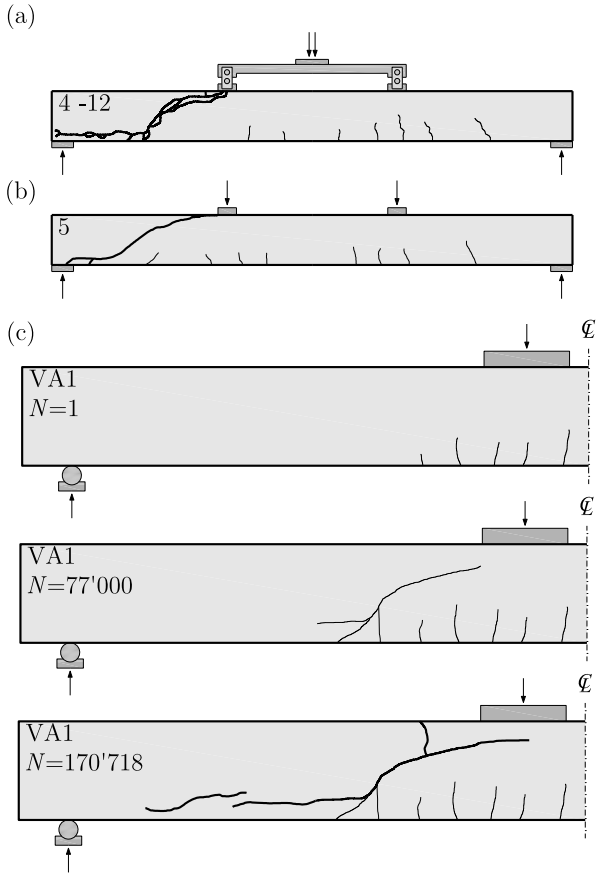


Fig. 2 Failure modes by Chang and Kesler (1958a,b): (a) shear-compression failure; (b) diagonal cracking failure; and Zanuy (2008): (c) cracking evolution and shear-compression failure.

1998; Johansson 2004) only showed some cases of shear fatigue failures after rebar fractures, being fatigue of the reinforcement the most common failure mode. A number of tests including shear fatigue failure tests was also carried out by other researchers that focused on details like the shape of the section (Frey and Thürlimann 1983; Markworth *et al*. 1984), the influence of large member size (Teng *et al*. 1984) or the effect of high strength concrete (Kwak and Park 2001). Despite the significant efforts devoted to experimental programmes, most codes of practice still ground their provisions on empirical formulas (CEN 2004, fib 2012).

With respect to the previous experimental experiences, it can be noted that shear fatigue failures are due to the development and growth of an eventually critical shear crack, leading to the loss of the beam shear-transfer actions strength (aggregate interlock, cantilever and dowelling action) (Higai 1978). Such failures are associated to members with moderate-to-high slenderness, where the shear strength depends on size and strain effects (governing the width of the critical shear crack (Muttoni and Ruiz 2008)). However, for low slender members, arching action is prevalent, which seems to be less prone to failures under shear fatigue (refer to Higai (1978), **Fig. 3**). Shear failures in these cases are associ-

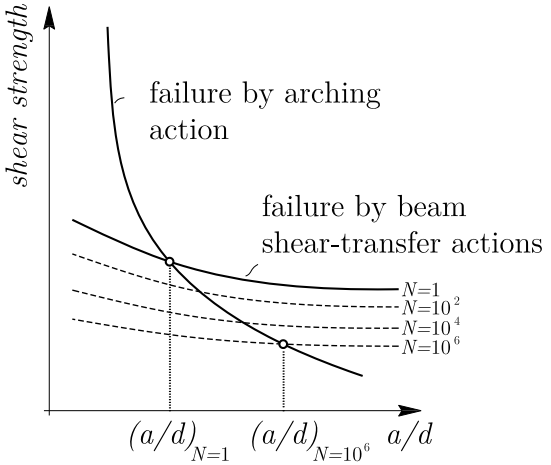


Fig. 3 Influence of fatigue loading on the shear strength of compact members (governed by arching action) and slender members (governed by beam shear-transfer actions).

ated to the crushing of the compression strut carrying shear, which is sensitive to strain effects (transverse strains) but where size effect (localization of strains on a single crack) plays a more limited role (Zhang and Tan 2007). This fact has recently been accounted by Gallego *et al*. (2014) that proposed a consistent approach for shear fatigue design of slender reinforced concrete members accounting for the development and growth of a critical shear crack based on fracture mechanics applied to quasi-brittle materials. This approach has shown to lead to consistent and accurate estimates of the fatigue shear strength (number of cycles leading to failure) and failure modes. Its application for practical purposes remains yet complex.

In this paper, the principles proposed by Gallego *et al*. (2014) are applied in combination with the Critical Shear Crack Theory. The latter aims at estimating the shear capacity of reinforced concrete members as a function of the opening and roughness of a critical shear crack leading to failure. The use of both approaches leads to simple design expressions, whose comparison to available test results shows sound agreement for the various mechanical and geometrical parameters. Also, both the S-N curves and Goodman diagrams for fatigue loading can be derived on an analytical manner, showing consistent agreement to test data, improving current empirical design formulas proposed by codes of practice (CEN 2004, fib 2012).

## 2. Existing design approaches for shear fatigue design

First attempts of developing design approaches for shear-fatigue failures were early developed by Chang and Kesler (1958a, b), who proposed a curve statistically obtained from their experimental tests in a semi-logarithmically S-N diagram ($V_{max}/V_{static}$ *vs* log$N$, where $V_{max}$ is the maximum applied load, $V_{static}$ the static strength load and $N$ the fatigue life). The proposal presented a threshold for a maximum applied load of about 60% of the static failure load. In a discussion of the works of Chang and Kesler, Taylor (1959) pointed out that the fatigue strength was not only influenced by the maximum applied load, but also by the ratio between minimum and maximum applied loads and the size of the members. These investigations were later followed by the works of Higai (1978) and Farghaly (1979) who proposed linear relationships in a semi-logarithmically S-N diagram without fatigue limits. One of the best known approaches was later established by Ueda (1982). Ueda (1982) proposed a S-N formulation acknowledging the influence of the quasi-static (monotonic) shear strength and the levels of shear loading:

$$\log\left(\frac{V_{max}}{V_{cu}}\right) = -0.036\left(1-\frac{V_{min}}{V_{max}}\left|\frac{V_{min}}{V_{max}}\right|\right)\log N \qquad (1)$$

where $V_{min}$ refers to the minimum applied shear force, $V_{max}$ to the maximum level of shear force and $V_{cu}$ to the quasi-static shear strength. This expression showed a reasonable fitting to test results and is even applicable to reverse shear loading, although comparisons to tests were not provided by the author in (Ueda 1982). The formula was proposed without a consistent demonstration based on rational models, but a physical discussion on the influencing parameters is available and its shape was derived following logical considerations (its constants being fitted on the basis of tests).

Codes of practice like Eurocode 2 (CEN 2004) or *fib*-Model Code 2010 (fib 2012) present shear-fatigue provisions for reinforced concrete members without shear reinforcement that are based on empirical Goodman diagrams or S-N formulations.

The Eurocode 2 distinguishes two different loading regimes. If the minimum ($V_{E,min}$) and maximum ($V_{E,max}$) applied shear forces have the same sign (no reverse loading), the code proposes for normal strength concrete (up to C50/60) the following Goodman diagram:

$$\frac{|V_{E,max}|}{|V_{R,c}|} \le 0.5 + 0.45\frac{|V_{E,min}|}{|V_{R,c}|} \le 0.9 \qquad (2)$$

where $V_{R,c}$ is the static shear strength. If the maximum and minimum shear forces do not have the same sign (reverse loading cases), Eq. (2) is modified as follows:

$$\frac{|V_{E,max}|}{|V_{d,c}|} \le 0.5 - \frac{|V_{E,min}|}{|V_{R,c}|} \qquad (3)$$

The proposed equation to calculate the static shear strength ($V_{Rd,c}$) in Eurocode 2 is based on an empirical formulation and not on a mechanical model. This equation can be found in Appendix A.

The *fib*-Model Code 2010 presents the following S-N formulation:

$$\log N \le 10\left(1-\frac{V_{\max}}{V_{\mathrm{Ref}}}\right) \tag{4}$$

where $V_{\max}$ is the maximum applied shear force, $V_{Ref}$ the static shear strength and $N$ the fatigue life. The static strength $V_{Ref}$ is calculated according to a mechanical model based on the Simplified Modified Compression Field Theory (Sigrist *et al*. 2013) and can be consulted in Appendix A. It can be noted that this formulation does not include any consideration on the level of minimum applied shear force (which has nevertheless been observed as a potentially significant parameter (Ueda 1982) and is explicitly incorporated by Eurocode 2). Eq. (4) was already included in the previous version of the Model Code, but with a different formulation for the estimate of the static strength.

Recently, a rational approach for shear fatigue has been proposed by Gallego *et al*. (2014). The fatigue strength is obtained as a result of the breakdown of resisting mechanisms due to the propagation of a shear crack. The model includes a two-parameter fracture mechanics-based propagation law, in which the stress intensity factor is evaluated at the tip of the effective shear crack. The model has allowed understanding the mechanics of the shear fatigue process, even though its application for practical purposes is not straightforward.

## 3. Consistent design for shear fatigue

In this section, the principles of Linear Elastic Fracture Mechanics (LEFM) applied to quasi-brittle materials together with the Paris-Erdogan law for crack propagation are briefly introduced, as they will be used to ground the proposed formulation for the shear strength of members subjected to fatigue loading. The analyses will be performed assuming also long-length cracks (as those characterizing shear failures). The validity of this assumption for concrete members failing in shear was previously investigated by Gallego *et al*. (2014).

According to LEFM, the propagation of a crack with the load cycles (d$a$/d$N$) depends on the amplitude of the stress intensity factor at the crack tip ($\Delta K$), refer to **Fig. 4**. Three regimes can then be distinguished: (a) initiation of crack propagation; (b) stable crack propagation; and (c) unstable crack propagation. The former is governed by a threshold ($\Delta K_0$) below which no propagation occurs. The latter leads to a fast an unstable crack propagation leading to failure. With respect to the stable crack propagation regime, it can be characterized by the empirical law observed by Paris-Erdogan (1963):

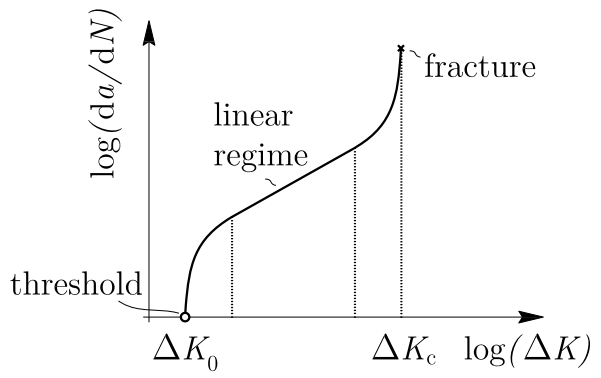


Fig. 4 Crack growth rate as a function of the stress intensity factor.

$$\frac{\mathrm{d}a}{\mathrm{d}N} = A\cdot\Delta K^{m} \tag{5}$$

where $A$ and $m$ are constants depending on the material properties. The validity of this law has been largely verified for metallic materials, with typical values for $A$ ranging between $3\cdot10^{-9}$ to $300\cdot10^{-9}$ and for $m$ ranging between 2.5 to 4.5. Applications to other materials (ceramic and plastic namely) has also been investigated. Also, values have been reported for granite (a material more similar to concrete), where the values of $A$ and $m$ result $2\cdot10^{-4}$ and 12 respectively (a detailed summary on suitable values can be consulted elsewhere (Elices Calafat 1998)).

For application to concrete, the Paris-Erdogan law has shown to provide suitable results provided that it incorporates the size effect factor (refer to Bažant and Xu 1991), which can be consistently introduced in the following manner:

$$\frac{\mathrm{d}a}{\mathrm{d}N} = C\cdot\left(\frac{\Delta K}{K_f}\right)^{m} \tag{6}$$

where $K_f$ refers to the fracture toughness. This expression can be transformed by considering the dependency of $K_f$ on the size of the element, expressed by means of brittleness number $\beta$ ($\beta = h/h_0$ where $h$ refers to the element representative size and $h_0$ to a constant) as (Bažant and Xu 1991):

$$\frac{\mathrm{d}a}{\mathrm{d}N} = C\cdot\left(\Delta\sigma\sqrt{(1+\beta)}\right)^{m} \tag{7}$$

Assuming, as a first approximation, that factors $\beta$ (related to size effect) and $C$ (depending on material and geometrical properties) are roughly constant (other assumptions could be adopted but will not be investigated hereafter), it is obtained by integration:

$$a-a_0 = C\cdot(1+\beta)^{m/2}\cdot\Delta\sigma^{m}N \tag{8}$$

where failure occurs for a crack $a = a_c$ at a number of cycles $N_R$, progressing from an initial crack length $a_0$. The expression thus turns into:

$$N_R = \frac{a_c-a_0}{C\cdot(1+\beta)^{m/2}\cdot\Delta\sigma^{m}} \tag{9}$$

Which can be rewritten as:

$$N_R^{1/m} = \frac{\left(\dfrac{a_c - a_0}{C \cdot (1+\beta)^{m/2}}\right)^{1/m}}{\Delta\sigma} \tag{10}$$

This equation provides the number of cycles required to lead to failure. Its direct evaluation is possible (Gallego *et al*. 2014), yet time-consuming and might be unpractical for simple design. Instead, the different terms can be correlated to physical values in the following manner:

- The stress amplitude can be assumed to be linearly dependent on the amplitude of the shear action, thus $\Delta\sigma \propto V_{c,N} - V_{\min}$, where $V_{c,N}$ refers to the shear force leading to failure at a number $N_R$ of cycles and $V_{\min}$ to the minimum acting shear force during the load cycles.
- The term on top of the fraction of Eq. (10) $((a_c - a_0)/(C \cdot (1+\beta)^{m/2}))^{1/m} \quad \left(= N_R^{1/m}\left(V_{c,N} - V_{\min}\right)\right)$ is assumed to be linearly dependent on the shear strength under monotonic loading minus the minimum acting shear force, thus: $((a_c - a_0)/(C \cdot (1+\beta)^{m/2}))^{1/m} \propto V_{c,1} - V_{\min}$.

It can be noted that the first hypothesis is reasonable and physically consistent, as the stresses acting in the member are proportional to the acting actions (provided that yielding of the reinforcement or crushing of concrete are not governing). Thus the acting range of stresses ($\Delta\sigma$) has to depend on the difference between maximum and minimum actions during load cycles ($V_{c,N} - V_{\min}$).

With respect to the second hypothesis, it is grounded on the fact that the crack length progresses from an initial length ($a_0$) to a critical one ($a_c$). This progression ($a_c - a_0$) takes place during a number of cycles $N$, when the applied shear force is increased (and thereafter decreased) in each cycle from a minimum acting shear force ($V_{\min}$) to a higher level. The critical length ($a_c$) can be assumed to be comparable to that developed by an identical member but loaded to failure in a monotonic manner (corresponding then to a shear force $V_{c,1}$). Thus, the increase of length of the crack from the minimum value during the load cycles to the critical one ($a_c - a_0$) could be related to the difference in the actions between the monotonic strength of the member and the minimum acting shear force during the load cycles ($V_{c,1} - V_{\min}$). The validity of this assumption can be easily verified for $N \to 1$, when $V_{\min} \to V_{c,1}$ leading to $a_0 \to a_c$. For other cases, its accuracy will be checked against available test results in the next section. It can be noted that future theoretical work is nevertheless required to assess or to correct the generality of this hypothesis.

With these two considerations, Eq. (10) turns to be:

$$N_R^{1/m} = \frac{V_{c,1} - V_{\min}}{V_{c,N} - V_{\min}}\kappa \tag{11}$$

The term $\kappa$ is a coefficient that accounts for the proportionality of the two terms $\left(V_{c,N} - V_{\min}\right.$ and $\left.V_{c,1} - V_{\min}\right)$. Its value can be obtained by means of comparison to test results. As it will be shown later, $\kappa = 1$ yields good predictions of the actual behavior and will be adopted in the following.

For the use of Eq. (11), it may also be noted that it is convenient to include by notation the term $R = V_{\min} / V_{c,N} \geq 0$, leading thus to:

$$\frac{V_{c,N}}{V_{c,1}} = \frac{1}{R + N_R^{1/m} \cdot (1-R)} \tag{12}$$

It can be noted that evaluation of Eq. (12) requires assessing the shear strength under monotonic loading (term $V_{c,1}$). This term depends on the material and geometrical parameters of the member and is influenced by some effects as size effect (refer to term $\beta$). For evaluation of this term, the Critical Shear Crack Theory (CSCT) (Muttoni and Ruiz 2008) can be used in a consistent manner. This theory considers a critical shear crack developing through the theoretical location of the compression strut carrying shear, refer to **Fig. 5**. The opening of the critical shear crack is estimated to be correlated to a reference strain (refer to **Figs. 5b-e** for location) times the effective depth of the member: $w \propto \varepsilon \cdot d$. On the basis of this assumption, the following failure criterion was proposed (Muttoni and Ruiz 2008) (equation in SI units [MPa, mm]):

$$\frac{V_{R,c}}{b \cdot d \sqrt{f_c}} = \frac{1}{6} \cdot \frac{2}{1 + 120 \dfrac{\varepsilon \cdot d}{16 + d_g}} \tag{13}$$

where $d_g$ refers to the maximum aggregate size, $f_c$ to the compressive strength of concrete measured in cylinders, $b$ to the width of the member and $d$ to its effective depth. This formulation has in-built the influence of size effect (referring to the effective depth on which the crack width relies) and considers the geometrical and mechanical parameters of the member in a consistent manner (Muttoni and Ruiz 2008). More details on how to apply the CSCT to beams without shear reinforcement can be found in Appendix A. The theory can also be used for members subjected to distributed loading (Pérez Caldentey *et al*. 2012) and when plastic strains develop in the flexural reinforcement (Vaz Rodrigues *et al*. 2010).

It should be noted that the CSCT is accepted valid for slender members ($a/d$>3) and in cases without reverse loading. These restrictions will thus be applied for the use of Eq. (12), and further studies should be performed to analyze its validity and potential modifications for these cases as well as other phenomena (like the damage accumulation (Palgrem-Miner effect)).

It can be noted also that the estimate of the monotonic shear strength $V_{c,1}$ incorporates already a number of

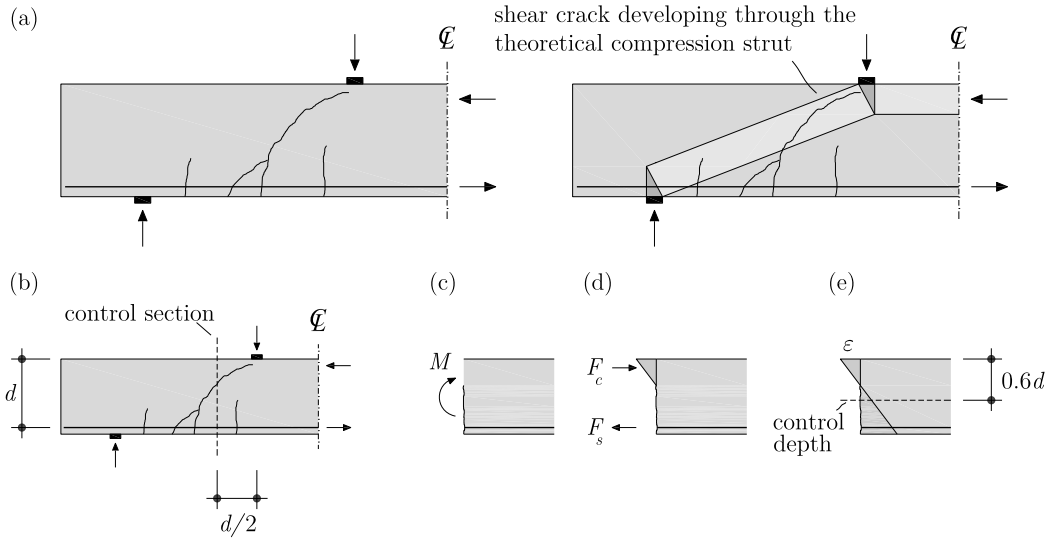


Fig. 5 Shear design according to the Critical Shear Crack Theory: (a) actual crack pattern and development of the critical shear crack through the theoretical location of the compression strut; (b) location of the control section; (c,d) bending moment in the control section; and (e) strains in the control section.

influences (size and strain effects, concrete and aggregate properties). In addition, the loading rate can also be considered to estimate the shear strength. The loading rate increases or decreases the concrete strength (Rüsch 1960; Ruiz *et al*. 2007) and this holds true also for shear-related failures under impact loading (Micallef *et al*. 2014) (with increasing nominal shear strength) or sustained loading (Sarkhosh *et al*. 2013) (with decreasing nominal shear strength).

## 4. Comparison to test results and existing design models

The previous design expression is compared in this section to the available experimental evidence. To that aim, the database presented in Gallego *et al*. (2014) will be used, considering only slender members ($a/d$ > 3) to avoid any arching action . The results are presented in terms both of S-N and Goodman diagrams.

It is to be noted that the loading rate is accounted for in the comparisons. This is justified as the quasi-static reference strength provided by the shear design formula of the CSCT (or other design models) is aimed at quasi-static failures in cases when loading duration is about one hour time (typical testing time). However, tests failing in fatigue loading are typically performed at much higher loading rates, typically 1 Hz. This implies that for $N_R \rightarrow 1$, the observed strength at higher loading rates should be higher than the corresponding one for a reference (quasi-static) specimen (Sarkhosh *et al*. 2013; Micallef *et al*. 2014). This phenomenon is accounted for in a simplified manner by using the Model Code 2010 expressions for modifying the concrete strength as a function of the loading rate (fib 2012). According to Model Code 2010, the increase on the concrete strength for tests performed at a loading rate of 1 Hz with respect to quasi-static specimens (1 hour-time for failure) is approximately 10% ($\eta = 1.10 \approx 3600^{0.014}$). This value will be accepted as affecting the monotonic shear strength $V_{c,1}$ although a more refined investigation of this parameter will require future work.

In addition, the threshold value for propagation of crack widths (refer to previous section) will be assumed as $V_{c,N}/V_{c,1}$ = 0.5 (the same as the one suggested by Eurocode 2 (CEN 2004)):

$$\frac{V_{c,N}}{V_{c,1}} = \frac{1}{R + N_R^{1/m} \cdot (1-R)} \geq 0.50 \tag{14}$$

**Figure 6** plots the results obtained with the proposed approach (Eq. (14)) compared to the available test dataset (Gallego et al. 2014). To that purpose, it has been proposed a value m = 17 and $\eta$ = 1.10. In addition, only tests with values of R lower than 10% have been selected. The influence of this parameter is investigated with the Goodman diagrams (**Fig. 7**). These values (m, $\eta$ and threshold) refer to the average response of the test results, and could be adapted, if necessary, to respect a target safety level (5% fractile or other). A very good agreement is obtained for this sub-set of tests, with an average ratio between $\left.\frac{V_{\max}}{V_{c,1}}\right|_{\text{test}}$ (Vc,1 calculated according to Eq. 13) and $\left.\frac{V_{c,N}}{V_{c,1}}\right|_{\text{model}}^{N}$ (substituting the experimental N in Eq. 14) equal to 1.06 with a CoV of 13%, refer to Table 1. It should be noted that the predictions show a very low scatter, with a value similar to that obtained by the CSCT for evaluation of monotonic shear failures (Muttoni and Ruiz 2008), thus the model for cyclic behavior adding no further scatter to the estimate of the shear strength. In addition, the threshold for shear

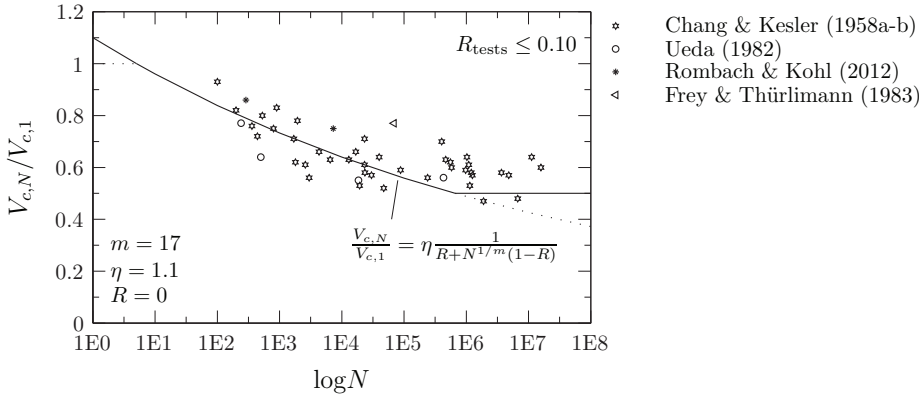


Fig. 6 Comparison of the proposed approach and available test data ($R$<10%) as a S-N diagram.

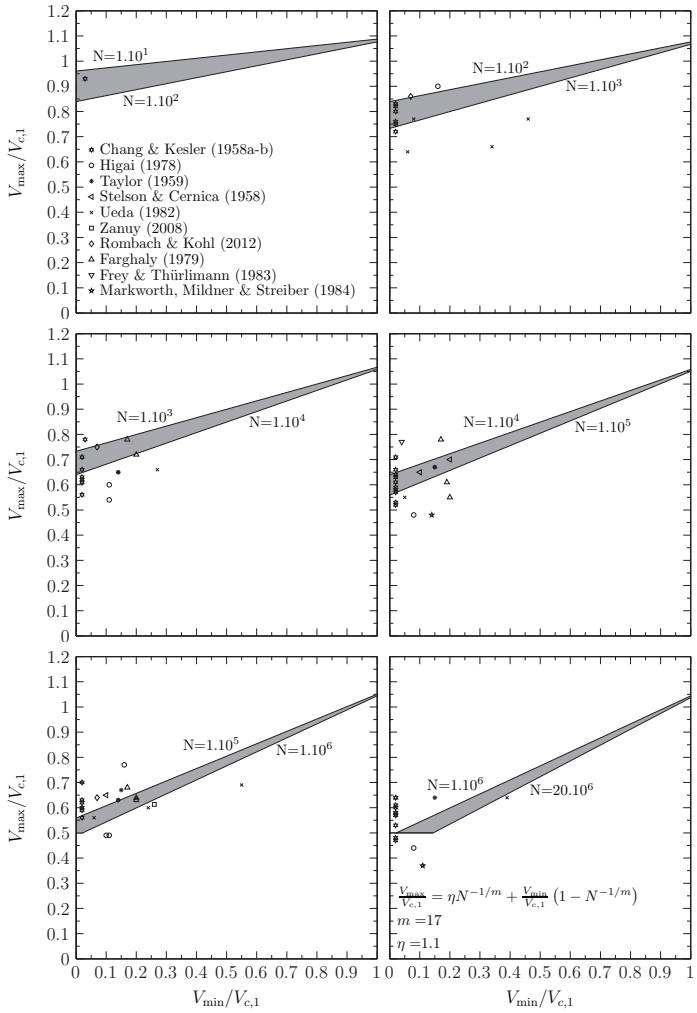


Fig. 7 Comparison of the proposed approach and available test data in Goodman diagrams.

crack propagation is attained for a number of cycles close to $10^6$.

The comparison of the test results in terms of Goodman diagrams allows observing the influence of the load levels ($V_{c,N}$ and $V_{\text{min}}$) on the shear fatigue strength. Such diagrams are shown in **Fig. 7** for the complete range $R$. The predictions are again consistent, suitably incorporating the influence of $R$. The results show a good agreement between the predicted and measured strengths (average equal to 1.00) with a low value of the CoV (15%), refer to **Table 1**. It can be noted that the value selected for the threshold is considered independent of the ratio $R$ in good agreement to test results. This aspect could however be developed in future research (for high values of parameter $R$, the specimen is permanently subjected to a high level of shear stresses, which may lead to the phenomenon of concrete fatigue under sustained loading (Ruiz *et al*. 2007)).

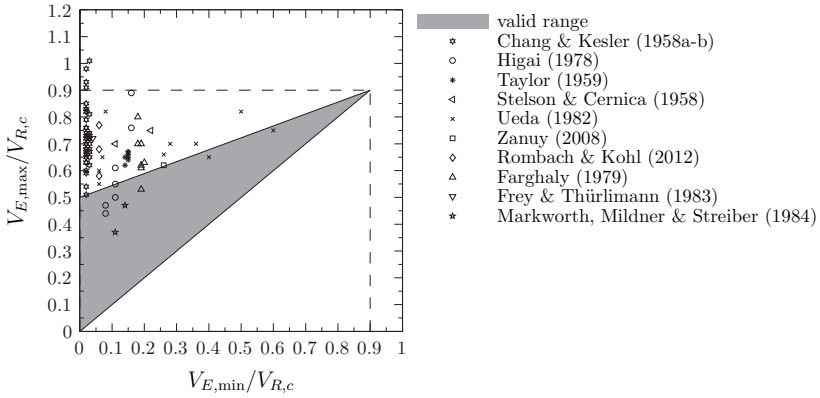


Fig. 8 Comparison of Eurocode 2 and available test data.

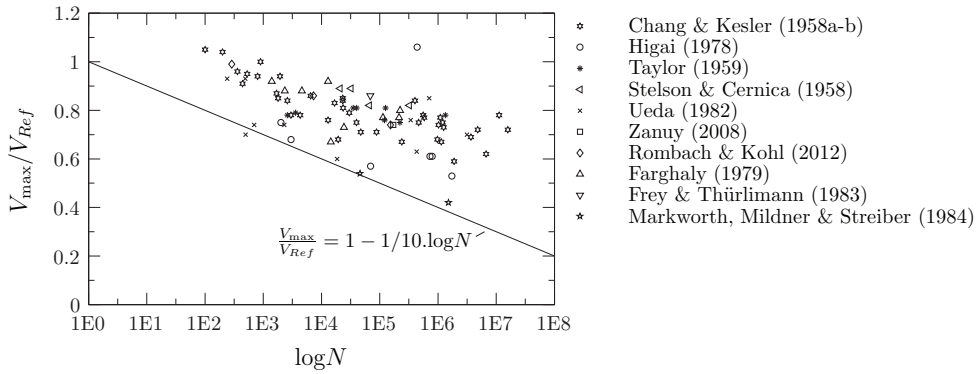


Fig. 9 Comparison of *fib*-Model Code 2010 and available test data.

With respect to codes of practice, it can be noted that the formulas of Eurocode 2 (refer to Eq. (2) and to Appendix A) are not an estimator of the number of cycles to failure, but they provide a suitable threshold to avoid premature shear failures. Its application to the database provides thus quite safe estimates of the shear fatigue failures (Average = 1.29, CoV = 0.20), refer to **Table 1** and to **Fig. 8**. With respect to Model Code 2010, (refer to Eq. (4) and to Appendix A), the formulation yields safe estimates (Average = 1.52, CoV = 0.22, as it should be expected for a design code), particularly for members failing under a large values of number of cycles, as it does not present any threshold, refer to **Table 1** and to **Fig. 9**. It can be noted that both design codes lead in fact to quite safe estimates on average but with significant scatter in the predictions. The test results are on the contrary well estimated with the proposed LEFM (for quasi-brittle materials) and the CSCT approach, with consistent and low scatter for both low and high number of cycles.

## 5. Conclusions

A consistent design approach for shear-fatigue of slender reinforced concrete members ($a/d > 3$) without transverse reinforcement is presented in this paper, applying the principles of Fracture Mechanics (FM) for quasi-brittle materials in combination with the Critical Shear Crack Theory (CSCT). The main conclusions of this paper are:

- Shear fatigue failures are due to development and growth of shear cracks. Consistent design can thus be performed on the basis of the FM for quasi-brittle materials combined with the CSCT. This approach leads to a simple, yet sound and rational, design equation incorporating the different influences of fatigue actions and shear strength:
  - minimum and maximum load levels
  - size and strain effects
  - material and geometrical properties
  - loading rate
- Shear-fatigue seems not to occur for values of maximum applied load below approximately 50% of the static shear strength, and this value can be satisfactorily used as a threshold for shear crack propagation when compared to test results (the number of tests with fatigue failure occurring at a number of cycles larger than $10^6$ cycles is yet limited).
- Consistent agreement is obtained with the proposed approach in terms of Wöhler (S-N) and Goodman diagrams, being the estimate of the number of cycles until failure significantly more accurate and with lower scatter than current empirical shear fatigue formulations of Eurocode 2 or *fib*-Model Code 2010. The scatter obtained with the proposed approach is in addition similar to that of the CSCT for members failing in shear under monotonic loading and thus the proposed formulation adds no further scatter to the phenomenon.

Table 1 Comparison between experimental tests and studied models.

| Experimental campaign | Test ID | $b$ (m) | $d$ (m) | $\rho_l$ (%) | $f_c$ (MPa) | $a/d$ | $d_g$ (mm) | $R$ | $V_{max}$ (kN) | experimental $N$ | Test to model ratio (1) CSCT $R$=0 (2) | CSCT $R$ (3) | MC2010 (4) | EC2 (5) |
|---|---|---|---|---|---|---|---|---|---|---|---|---|---|---|
| Chang & Kesler (1958a-b) | 2 | 0.10 | 0.14 | 1.02 | 42.7 | 3.7 | 25 | 0.04 | 12 | 23500 | 0.96 | 0.94 | 1.44 | 1.37 |
| Chang & Kesler (1958a-b) | 3 | 0.10 | 0.14 | 1.02 | 41.2 | 3.7 | 25 | 0.04 | 12 | 3000 | 0.82 | 0.81 | 1.19 | 1.32 |
| Chang & Kesler (1958a-b) | 4 | 0.10 | 0.14 | 1.02 | 34.1 | 3.7 | 25 | 0.04 | 12 | 6500 | 0.96 | 0.95 | 1.40 | 1.47 |
| Chang & Kesler (1958a-b) | 5 | 0.10 | 0.14 | 1.02 | 36.2 | 3.7 | 25 | 0.04 | 12 | 1800 | 0.87 | 0.86 | 1.26 | 1.44 |
| Chang & Kesler (1958a-b) | 9 | 0.10 | 0.14 | 1.02 | 36.9 | 3.7 | 25 | 0.04 | 12 | 2600 | 0.88 | 0.87 | 1.28 | 1.43 |
| Chang & Kesler (1958a-b) | 10 | 0.10 | 0.14 | 1.02 | 30.5 | 3.7 | 25 | 0.05 | 10 | 47100 | 0.90 | 0.88 | 1.34 | 1.21 |
| Chang & Kesler (1958a-b) | 12 | 0.10 | 0.14 | 1.02 | 38.3 | 3.7 | 25 | 0.04 | 12 | 23200 | 1.00 | 0.99 | 1.49 | 1.42 |
| Chang & Kesler (1958a-b) | 22 | 0.10 | 0.14 | 1.02 | 44.1 | 3.7 | 25 | 0.04 | 12 | 30000 | 0.95 | 0.93 | 1.44 | 1.34 |
| Chang & Kesler (1958a-b) | 4-6 | 0.10 | 0.14 | 1.86 | 29.3 | 3.7 | 25 | 0.03 | 16 | 800 | 1.00 | 1.00 | 1.33 | 1.62 |
| Chang & Kesler (1958a-b) | 4-7 | 0.10 | 0.14 | 1.86 | 32.1 | 3.7 | 25 | 0.02 | 18 | 200 | 1.02 | 1.01 | 1.36 | 1.80 |
| Chang & Kesler (1958a-b) | 4-8 | 0.10 | 0.14 | 1.86 | 32.0 | 3.7 | 25 | 0.03 | 13 | 557000 | 1.22 | 1.20 | 1.84 | 1.35 |
| Chang & Kesler (1958a-b) | 4-9 | 0.10 | 0.14 | 1.86 | 27.0 | 3.7 | 25 | 0.03 | 13 | 16800 | 1.07 | 1.05 | 1.44 | 1.43 |
| Chang & Kesler (1958a-b) | 4-11 | 0.10 | 0.14 | 1.86 | 27.2 | 3.7 | 25 | 0.05 | 10 | 1900200 | 0.94 | 0.94 | 1.58 | 1.01 |
| Chang & Kesler (1958a-b) | 4-12 | 0.10 | 0.14 | 1.86 | 29.6 | 3.7 | 25 | 0.04 | 11 | 1142100 | 1.06 | 1.06 | 1.70 | 1.15 |
| Chang & Kesler (1958a-b) | 4-14 | 0.10 | 0.14 | 1.86 | 37.3 | 3.7 | 25 | 0.04 | 12 | 19300 | 0.86 | 0.85 | 1.19 | 1.17 |
| Chang & Kesler (1958a-b) | 4-15 | 0.10 | 0.14 | 1.86 | 14.8 | 3.7 | 25 | 0.04 | 12 | 1940 | 1.11 | 1.09 | 1.39 | 1.59 |
| Chang & Kesler (1958a-b) | 4-16 | 0.10 | 0.14 | 1.86 | 29.2 | 3.7 | 25 | 0.03 | 15 | 440 | 0.94 | 0.93 | 1.24 | 1.57 |
| Chang & Kesler (1958a-b) | 4-17 | 0.10 | 0.14 | 1.86 | 29.6 | 3.7 | 25 | 0.03 | 16 | 360 | 0.97 | 0.96 | 1.28 | 1.65 |
| Chang & Kesler (1958a-b) | 4-19 | 0.10 | 0.14 | 1.86 | 35.9 | 3.7 | 25 | 0.04 | 11 | 6690200 | 0.97 | 0.97 | 1.95 | 1.06 |
| Chang & Kesler (1958a-b) | 4-24 | 0.10 | 0.14 | 1.86 | 31.7 | 3.7 | 25 | 0.04 | 12 | 4822400 | 1.14 | 1.14 | 2.17 | 1.24 |
| Chang & Kesler (1958a-b) | 4-25 | 0.10 | 0.14 | 1.86 | 29.5 | 3.7 | 25 | 0.04 | 13 | 1097300 | 1.21 | 1.21 | 1.93 | 1.31 |
| Chang & Kesler (1958a-b) | 4-27 | 0.10 | 0.14 | 1.86 | 35.3 | 3.7 | 25 | 0.03 | 13 | 1250400 | 1.14 | 1.14 | 1.86 | 1.25 |
| Chang & Kesler (1958a-b) | 4-28 | 0.10 | 0.14 | 1.86 | 37.4 | 3.7 | 25 | 0.03 | 14 | 578800 | 1.20 | 1.18 | 1.83 | 1.33 |
| Chang & Kesler (1958a-b) | 4-29 | 0.10 | 0.14 | 1.86 | 37.0 | 3.7 | 25 | 0.03 | 13 | 1207600 | 1.16 | 1.16 | 1.91 | 1.28 |
| Chang & Kesler (1958a-b) | 1-5 | 0.10 | 0.14 | 2.89 | 19.9 | 3.7 | 25 | 0.04 | 12 | 1027200 | 1.28 | 1.28 | 1.86 | 1.41 |
| Chang & Kesler (1958a-b) | 2-5 | 0.10 | 0.14 | 2.89 | 19.7 | 3.7 | 25 | 0.04 | 11 | 976100 | 1.17 | 1.17 | 1.69 | 1.28 |
| Chang & Kesler (1958a-b) | 3-5 | 0.10 | 0.14 | 2.89 | 25.0 | 3.7 | 25 | 0.03 | 13 | 467200 | 1.24 | 1.22 | 1.72 | 1.43 |
| Chang & Kesler (1958a-b) | 5-3 | 0.10 | 0.14 | 2.89 | 32.6 | 3.7 | 25 | 0.03 | 17 | 23200 | 1.16 | 1.14 | 1.51 | 1.64 |
| Chang & Kesler (1958a-b) | 5-4 | 0.10 | 0.14 | 2.89 | 37.0 | 3.7 | 25 | 0.02 | 18 | 1700 | 1.00 | 1.00 | 1.28 | 1.68 |
| Chang & Kesler (1958a-b) | 5-5 | 0.10 | 0.14 | 2.89 | 32.2 | 3.7 | 25 | 0.03 | 16 | 402900 | 1.36 | 1.34 | 1.91 | 1.62 |
| Chang & Kesler (1958a-b) | 5-6 | 0.10 | 0.14 | 2.89 | 34.7 | 3.7 | 25 | 0.03 | 14 | 15871700 | 1.19 | 1.19 | 2.57 | 1.39 |
| Chang & Kesler (1958a-b) | 5-3 | 0.10 | 0.14 | 2.89 | 34.5 | 3.7 | 25 | 0.03 | 16 | 11217700 | 1.29 | 1.29 | 2.63 | 1.50 |
| Chang & Kesler (1958a-b) | 5-10 | 0.10 | 0.14 | 2.89 | 14.9 | 3.7 | 25 | 0.03 | 16 | 100 | 1.11 | 1.10 | 1.31 | 1.99 |
| Chang & Kesler (1958a-b) | 5-11 | 0.10 | 0.14 | 2.89 | 24.8 | 3.7 | 25 | 0.03 | 13 | 39800 | 1.08 | 1.06 | 1.39 | 1.43 |
| Chang & Kesler (1958a-b) | 5-12 | 0.10 | 0.14 | 2.89 | 28.0 | 3.7 | 25 | 0.02 | 18 | 530 | 1.06 | 1.05 | 1.31 | 1.84 |
| Chang & Kesler (1958a-b) | 5-13 | 0.10 | 0.14 | 2.89 | 30.6 | 3.7 | 25 | 0.03 | 13 | 3666500 | 1.16 | 1.16 | 2.02 | 1.34 |
| Chang & Kesler (1958a-b) | 5-14 | 0.10 | 0.14 | 2.89 | 36.8 | 3.7 | 25 | 0.03 | 16 | 13000 | 0.99 | 0.98 | 1.29 | 1.47 |
| Chang & Kesler (1958a-b) | 5-15 | 0.10 | 0.14 | 2.89 | 33.2 | 3.7 | 25 | 0.03 | 13 | 239000 | 1.06 | 1.04 | 1.46 | 1.30 |
| Chang & Kesler (1958a-b) | 5-16 | 0.10 | 0.14 | 2.89 | 27.6 | 3.7 | 25 | 0.03 | 14 | 4300 | 0.98 | 0.97 | 1.23 | 1.50 |
| Chang & Kesler (1958a-b) | 5-17 | 0.10 | 0.14 | 2.89 | 35.8 | 3.7 | 25 | 0.03 | 14 | 87800 | 1.04 | 1.03 | 1.41 | 1.38 |
| Chang & Kesler (1958a-b) | 5-20 | 0.10 | 0.14 | 2.89 | 32.7 | 3.7 | 25 | 0.02 | 20 | 900 | 1.13 | 1.12 | 1.42 | 1.94 |
| Stelson & Cernica (1958) | 1 | 0.13 | 0.11 | 2.90 | 26.6 | 5.6 | 13 | 0.15 | 13 | 66000 | - | 1.05 | 1.59 | 1.30 |
| Stelson & Cernica (1958) | 2 | 0.13 | 0.11 | 2.90 | 26.6 | 5.6 | 13 | 0.15 | 13 | 323000 | - | 1.14 | 1.83 | 1.30 |
| Stelson & Cernica (1958) | 7 | 0.13 | 0.11 | 2.90 | 26.6 | 5.6 | 13 | 0.29 | 14 | 32000 | - | 1.01 | 1.61 | 1.31 |
| Stelson & Cernica (1958) | 8 | 0.13 | 0.11 | 2.90 | 26.6 | 5.6 | 13 | 0.29 | 14 | 20800 | - | 0.99 | 1.56 | 1.31 |
| Taylor (1959) | 2 | 0.19 | 0.22 | 1.21 | 29.5 | 4.1 | 19 | 0.23 | 31 | 1340000 | - | 1.16 | 2.02 | 1.14 |
| Taylor (1959) | 3 | 0.19 | 0.22 | 1.21 | 29.5 | 4.1 | 19 | 0.22 | 33 | 40000 | - | 1.02 | 1.50 | 1.20 |
| Taylor (1959) | 5 | 0.19 | 0.22 | 1.49 | 29.5 | 4.1 | 19 | 0.22 | 35 | 126000 | - | 1.09 | 1.66 | 1.20 |
| Taylor (1959) | 6 | 0.19 | 0.22 | 1.49 | 29.5 | 4.1 | 19 | 0.22 | 35 | 35000 | - | 1.02 | 1.49 | 1.20 |
| Taylor (1959) | 9 | 0.19 | 0.22 | 1.83 | 29.5 | 4.1 | 19 | 0.22 | 35 | 121000 | - | 1.02 | 1.54 | 1.12 |
| Taylor (1959) | 10 | 0.19 | 0.22 | 1.83 | 29.5 | 4.1 | 19 | 0.21 | 36 | 3600 | - | 0.88 | 1.22 | 1.17 |
| Taylor (1959) | 13 | 0.19 | 0.22 | 2.33 | 29.5 | 4.1 | 19 | 0.23 | 38 | 222000 | - | 1.04 | 1.62 | 1.16 |
| Taylor (1959) | 14 | 0.19 | 0.22 | 2.33 | 29.5 | 4.1 | 19 | 0.22 | 39 | 2600 | - | 0.86 | 1.18 | 1.21 |
| Higai (1978) | FT 3 | 0.20 | 0.20 | 2.15 | 39.8 | 4.0 | 15 (*) | 0.19 | 27 | 1740000 | - | 0.83 | 1.40 | 0.80 |
| Higai (1978) | FT 4 | 0.20 | 0.20 | 2.15 | 39.8 | 4.0 | 15 (*) | 0.17 | 29 | 70000 | - | 0.77 | 1.11 | 0.88 |
| Higai (1978) | FT 13 | 0.20 | 0.16 | 2.40 | 31.1 | 5.0 | 15 (*) | 0.18 | 28 | 2000 | - | 0.80 | 1.12 | 1.12 |
| Higai (1978) | FT 14 | 0.20 | 0.16 | 2.40 | 29.1 | 5.0 | 15 (*) | 0.20 | 25 | 3000 | - | 0.73 | 1.04 | 1.00 |
| Higai (1978) | FT 16 | 0.20 | 0.16 | 2.40 | 32.8 | 5.0 | 15 (*) | 0.22 | 23 | 790000 | - | 0.87 | 1.49 | 0.90 |
| Higai (1978) | FT 19 | 0.20 | 0.16 | 2.40 | 35.1 | 5.0 | 15 (*) | 0.21 | 24 | 730000 | - | 0.87 | 1.47 | 0.90 |
| Higai (1978) | FT 6 | 0.20 | 0.11 | 1.80 | 34.4 | 6.4 | 15 (*) | 0.18 | 28 | 500 | - | 1.12 | 1.71 | 1.64 |
| Higai (1978) | FT 7 | 0.20 | 0.11 | 1.80 | 35.5 | 6.4 | 15 (*) | 0.21 | 24 | 440000 | - | 1.33 | 2.44 | 1.38 |
| Farghaly (1979) | 3.5-F-70-1 | 0.30 | 0.22 | 1.74 | 30.1 | 3.5 | 20 (*) | 0.31 | 55 | 24300 | - | 0.87 | 1.30 | 1.09 |
| Farghaly (1979) | 3.5-F-70-2 | 0.30 | 0.22 | 1.74 | 22.5 | 3.5 | 20 (*) | 0.25 | 55 | 223500 | - | 1.11 | 1.73 | 1.24 |
| Farghaly (1979) | 3.5-F-80-1 | 0.30 | 0.22 | 1.74 | 22.5 | 3.5 | 20 (*) | 0.22 | 63 | 1400 | - | 1.01 | 1.34 | 1.44 |
| Farghaly (1979) | 3.5-F-80-2 | 0.30 | 0.22 | 1.74 | 22.5 | 3.5 | 20 (*) | 0.22 | 63 | 13000 | - | 1.12 | 1.57 | 1.44 |
| Farghaly (1979) | 4.5-F-60-1 | 0.30 | 0.22 | 1.74 | 26.0 | 4.5 | 20 (*) | 0.36 | 44 | 14500 | - | 0.74 | 1.14 | 0.89 |
| Farghaly (1979) | 4.5-F-70-1 | 0.30 | 0.22 | 1.74 | 26.0 | 4.5 | 20 (*) | 0.31 | 51 | 214000 | - | 1.00 | 1.65 | 1.06 |

| | | | | | | | | | | | | Test to model ratio (1) | | | |
|---|---|---|---|---|---|---|---|---|---|---|---|---|---|---|---|
| Experimental campaign | Test ID | $b$ (m) | $d$ (m) | $\rho_l$ (%) | $f_c$ (MPa) | $a/d$ | $d_g$ (mm) | $R$ | $V_{max}$ (kN) | experimental $N$ | CSCT $R$=0 (2) | CSCT $R$ (3) | MC2010 (4) | EC2 (5) |
| Farghaly (1979) | 4.5-F-70-2 | 0.30 | 0.22 | 1.74 | 26.3 | 4.5 | 20 (*) | 0.31 | 51 | 113700 | - | 0.97 | 1.56 | 1.06 |
| Farghaly (1979) | 4.5-F-80-1 | 0.30 | 0.22 | 1.74 | 26.0 | 4.5 | 20 (*) | 0.28 | 58 | 2350 | - | 0.93 | 1.33 | 1.23 |
| Farghaly (1979) | 4.5-F-80-2 | 0.30 | 0.22 | 1.74 | 26.3 | 4.5 | 20 (*) | 0.28 | 58 | 4600 | - | 0.96 | 1.38 | 1.22 |
| Ueda (1982) | 1A | 0.20 | 0.44 | 0.68 | 33.4 | 3.5 | 25 | 0.10 | 49 | 500 | 0.84 | 0.81 | 0.96 | 1.25 |
| Ueda (1982) | 1B | 0.20 | 0.44 | 0.68 | 33.4 | 3.5 | 25 | 0.61 | 49 | 3140000 | - | 0.90 | 2.01 | 0.95 |
| Ueda (1982) | 2A | 0.20 | 0.44 | 0.68 | 45.5 | 3.5 | 25 | 0.10 | 46 | 18600 | 0.89 | 0.85 | 1.05 | 1.06 |
| Ueda (1982) | 3B | 0.20 | 0.44 | 1.67 | 33.4 | 3.5 | 25 | 0.51 | 71 | 700 | - | 0.74 | 1.04 | 1.08 |
| Ueda (1982) | 4A | 0.20 | 0.44 | 1.67 | 45.5 | 3.5 | 25 | 0.10 | 67 | 430000 | 1.10 | 1.04 | 1.45 | 1.14 |
| Ueda (1982) | 4B | 0.20 | 0.44 | 1.67 | 45.5 | 3.5 | 25 | 0.41 | 79 | 2300 | - | 0.81 | 1.12 | 1.15 |
| Ueda (1982) | 5B | 0.40 | 0.22 | 0.68 | 34.2 | 3.5 | 25 | 0.40 | 58 | 341000 | - | 0.91 | 1.71 | 1.08 |
| Ueda (1982) | 7A | 0.40 | 0.22 | 1.67 | 34.2 | 3.5 | 25 | 0.60 | 98 | 490 | - | 0.82 | 1.28 | 1.20 |
| Ueda (1982) | 7B | 0.40 | 0.22 | 1.67 | 34.2 | 3.5 | 25 | 0.10 | 98 | 240 | 0.96 | 0.94 | 1.23 | 1.57 |
| Ueda (1982) | 8A | 0.40 | 0.22 | 1.67 | 46.0 | 3.5 | 25 | 0.80 | 99 | 706000 | - | 0.79 | 2.06 | 0.96 |
| Frey & Thürlimann (1983) | BII-7 | 0.30 | 0.37 | 1.72 | 32.3 | 4.3 | 16 | 0.05 | 95 | 69000 | 1.35 | 1.31 | 1.67 | 1.41 |
| Markworth, Mildner & Streiber (1984) | H2-4 | 0.30 | 0.30 | 0.84 | 40.0 | 3.5 | 16 | 0.30 | 45 | 46000 | - | 0.70 | 1.01 | 0.82 |
| Markworth, Mildner & Streiber (1984) | H2-5 | 0.30 | 0.30 | 0.84 | 40.0 | 3.5 | 16 | 0.30 | 35 | 1512000 | - | 0.65 | 1.10 | 0.64 |
| Zanuy (2008) | VA1 | 0.30 | 0.26 | 2.51 | 25.0 | 5.2 | 20 | 0.42 | 60 | 170718 | - | 0.89 | 1.55 | 1.00 |
| Rombach & Kohl (2012) | V-3 | 0.20 | 0.30 | 1.57 | 39.0 | 5.0 | 16 | 0.08 | 60 | 289 | 1.09 | 1.06 | 1.31 | 1.49 |
| Rombach & Kohl (2012) | V-4 | 0.20 | 0.30 | 1.57 | 39.0 | 5.0 | 16 | 0.10 | 53 | 7290 | 1.15 | 1.11 | 1.40 | 1.30 |
| Rombach & Kohl (2012) | V-5 | 0.20 | 0.30 | 1.57 | 39.0 | 5.0 | 16 | 0.11 | 45 | 153000 | - | 1.11 | 1.53 | 1.10 |
| | | | | | | | | | | AVG | 1.06 | 1.00 | 1.52 | 1.29 |
| | | | | | | | | | | CoV | 0.13 | 0.15 | 0.22 | 0.20 |

Note: (1) ratio $\left.\dfrac{\dfrac{V_{max}}{V_{R,c}^{model}}\right|_{test}}{\left.\dfrac{V_{max}}{V_{R,c}}\right|_{model}^{N}}$; (2) $\left.\dfrac{V_{c,N}}{V_{c,1}}\right|_{model}^{N} = \eta N^{-1/m}$; (3) $\left.\dfrac{V_{c,N}}{V_{c,1}}\right|_{model}^{N} = \eta \dfrac{1}{R + N^{1/m}(1-R)}$;

(4) $\left.\dfrac{V_{max}}{V_{Ref}}\right|_{model}^{N} = 1 - \dfrac{1}{10}\log N$; (5) $\left.\dfrac{V_{max}}{V_{R,c}}\right|_{model}^{N} = \dfrac{0.5}{1-0.45R}$

## References


Bažant, Z. P. and Xu, K., (1991). "Size effect in fatigue fracture of concrete." *ACI Materials Journal*, 88(4), 390-399.

CEN European Committee for Standardization, (2004). "*Eurocode 2 - Design of concrete structures – Part 1-1: General rules and rules for buildings.*" Brussels, December, 225p.

Chang T. S. and Kesler C. E., (1958a). "Static and fatigue strength in shear of beams with tensile reinforcement." *ACI Journal*, 54(6), 1033-1057.

Chang T. S and Kesler C. E., (1985b). "Fatigue behaviour of reinforced concrete beams." *ACI Journal*, 55(8), 245-254.

Elices Calafat, M., (1998) "*Fracture mechanics applied to 2-D elastic bodies*." Lecture notes, ETSICCP – Universidad Politécnica de Madrid, 94 p. (in Spanish)

Farghaly, S. A., (1979). "*Shear design of reinforced concrete beams for static and repeated loads*." Doctoral Thesis, University of Tokyo. (in Japanese)

Fédération Internationale du Béton (fib), (2012). "*Model Code 2010 - Final draft.*" Bulletins 65 and 66, Lausanne, Switzerland, Vols. 1 and 2, 350 p. and 370 p.

Fernández Ruiz, M., Muttoni, A., and Gambarova, P. G., (2007). "Relationship between nonlinear creep and cracking of concrete under uniaxial compression." *Journal of Advanced Concrete Technology*, 5(3), 383-393.

Frey, R. and Thürlimann, B., (1983). "*Fatigue tests on reinforced concrete beams with and without shear reinforcement.*" Institut für Baustatik und Konstruktion ETHZ, Zurich, Switzerland. (in German)

Gallego, J. M., Zanuy, C. and Albajar, L., (2014). "Shear fatigue behaviour of reinforced concrete elements without shear reinforcement." *Engineering Structures*, 79, 45-57.

Higai, T., (1978). "*Fundamental study on shear failure of reinforced concrete beams*." *Proceedings of the Japan Society of Civil Engineers (JSCE)*, 1(279), 113-126.

Johansson, U., (2004). "*Fatigue tests and analysis of reinforced concrete bridge deck models*." Licentiate Thesis, Royal Institute of Technology, Stockholm, Sweden.

Kwak, K. H. and Park, J. G., (2001). "Shear-fatigue behaviour of high-strength reinforced concrete beams under repeated loading." *Structural Engineering and Mechanics*, 11(3), 301-314.

Markworth, E., Mildner, K. and Streiber, A., (1984). "Tests on shear strength of reinforced concrete beams

under dynamic loading." *Die Strasse*, 6, 175-180. (in German)

Micallef, K., Sagaseta, J., Fernández Ruiz, M. and Muttoni, A., (2014). "Assessing punching shear failure in reinforced concrete flat slabs subjected to localized impact loading." *International Journal of Impact Engineering*, 71, 17-33.

Muttoni, A. and Fernández Ruiz, M., (2008). "Shear strength of members without transverse reinforcement as function of critical shear crack width." *ACI Structural Journal*, 105(2), 163-172.

Natário, F. and Muttoni, A., (2014). "Static and fatigue strength of RC slabs under concentrated loads near linear supports." *Proc. of the 10th fib International PhD Symposium in Civil Engineering*, Quebec, Canada, 449-454.

Paris, P. C. and Erdogan, F., (1963). "A critical analysis of crack propagation laws." *Tans. ASME, J. Basic Eng.*, 85, p528-533.

Pérez Caldentey, A., Padilla, P., Muttoni, A. and Fernández Ruiz, M., (2012). "Effect of load distribution on the shear resistance of RC elements without stirrups." *ACI Structural Journal*, 109(5), 595-603.

Rombach, G. and Kohl, M., (2012). "Resistance of concrete members without shear reinforcement to fatigue loads." *Congress of IABSE*.

Rombach, G., Kohl, M. (2013). "Shear design of reinforced concrete bridge deck slabs according to Eurocode 2." *Journal of Bridge Engineering*, 18, 1261-1269.

Rüsch, H., (1960). "Research toward a general flexural theory for structural concrete." *ACI Journal*, 57(1), 1-28.

Sarkhosh, R., Walraven, J. C., den Uijl, J. A. and Braam, C. R., (2013). "Shear capacity of concrete beams under sustained loading." *Assessment, Upgrading and Refurbishment of Infrastructures IABSE Conference*, Rotterdam, the Netherlands.

Schläfli, M. and Brühwiler, E., (1998). "Fatigue of existing reinforced concrete bridge deck slabs." *Engineering Structures*, 20(11), 991-998.

Sigrist, V., Bentz, E., Fernández Ruiz, M., Foster, S. and Muttoni, A., (2013). "Background to the fib Model Code 2010 shear provisions - part I: beams and slabs." *Structural Concrete*, 14(3), 204-214.

Stelson, T. E. and Cernica, J. N., (1958). "Fatigue properties of concrete beams." *ACI Journal Proceeding*, 55(8), 255-259.

Taylor, R., (1959). "Discussion of a Paper by Chang T.S and Kesler C. E. Fatigue behaviour of reinforced concrete beams." *ACI Journal*, 55(14), 1011-1015.

Teng, S., Ma, W., Tan, K. H. and Kong, F. K., (1984). "Fatigue tests of reinforced concrete deep beams." *The Structural Engineer*, 76(18), 347-352.

Ueda, T., (1982). "*Behaviour in shear of reinforced concrete beams under fatigue loading.*" Doctoral Thesis, University of Tokyo.

Vaz Rodrigues, R., Muttoni, A. and Fernández Ruiz, M., (2010). "Influence of shear on rotation capacity of reinforced concrete members wthout shear reinforcement." *ACI Structural Journal*, 107(5), 516-525.

Verna, J. R. and Stelson, T. E., (1962). "Failure of small reinforced concrete beams under repeated loads." *ACI Journal Proceedings*, 59(10), 1489-1504.

Zanuy, C., (2008). "*Sectional analysis of reinforced concrete elements subjected to fatigue, including sections between cracks.*" Universidad Politécnica de Madrid, 251p. (in Spanish)

Zhang, N. and Tan, K.-H., (2007). "Size effect in RC deep beams: Experimental investigation and STM verification." *Engineering Structures*, 29(12), 3241-3254.

## Appendix: Notation

| | |
|---|---|
| $a$ | shear span (distance between the center of the load and the center of the support) |
| $a$ | crack length |
| $a_0$ | initial crack length |
| $a_c$ | critical crack length |
| $b$ | beam width |
| $b_w$ | beam width |
| $c$ | depth of compression zone |
| $d$ | effective flexural depth |
| $d_g$ | maximum aggregate size |
| $\mathrm{d}a/\mathrm{d}N$ | rate of crack length propagation with loading cycles |
| $f_c$ | concrete compressive strength measured in cylinders |
| $h$ | element representative size |
| $h_0$ | constant |
| $m$ | constant |
| $z$ | effective shear depth |
| $A$ | constant |
| $C$ | constant |
| $E_c$ | reinforcement modulus of concrete |
| $E_s$ | reinforcement modulus of elasticity |
| $K_f$ | fracture toughness |
| $M$ | acting bending moment |
| $M_E$ | acting bending moment |
| $N$ | fatigue life |
| $N_R$ | fatigue life |
| $P_{\max}$ | maximum applied load |
| $P_{\text{static}}$ | static strength load |
| $R$ | ratio between minimum and maximum applied loads |
| $V$ | acting shear force |
| $V_{c,1}$ | static shear strength for monotonic loading |
| $V_{cu}$ | static shear strength |
| $V_{c,N}$ | applied fatigue shear force |
| $V_{\text{E,max}}$ | maximum shear force |
| $V_{\text{E,min}}$ | minimum shear force |
| $V_{\max}$ | maximum shear force |
| $V_{\min}$ | minimum shear force |
| $V_{R,c}$ | static shear strength |
| $V_{Ref}$ | static shear strength |

$\beta$ brittleness number
$\varepsilon$ reference strain at $0.6d$ from the compressive face
$\varepsilon_x$ reference strain at mid-depth of the effective shear depth
$\kappa$ proportionality factor
$\eta$ multiplying factor of static strength due loading rate
$\rho$ reinforcement ratio
$\rho_l$ reinforcement ratio
$\Delta\sigma$ variation of stress
$\Delta K$ variation of stress intensity factor
$\Delta K_0$ propagation threshold of the variation of stress intensity factor
$\Delta K_c$ critical variation of stress intensity factor
$\Delta V$ variation of shear force

## Appendix A

The applied formulations used in this paper to calculate the static shear strength of reinforced concrete rectangular beams without shear and skin reinforcement are presented in this appendix

### A1) Shear strength according to the Critical Shear Crack Theory

If no axial force is applied, the strain $\varepsilon$ in the control depth at the control section depends on the applied bending moment $M$ as follows:

$$\varepsilon = \frac{M}{bd\rho E_s\left(d-c/3\right)}\frac{0.6d-c}{d-c} \tag{15}$$

where $b$ represents the width of the beam, $d$ the effective depth, $\rho$ the reinforcement ratio and $E_s$ the reinforcement modulus of elasticity. The depth of the compression zone $c$ is given by:

$$c = d\rho\frac{E_s}{E_c}\left(\sqrt{1+\frac{2E_c}{\rho E_s}}-1\right) \tag{16}$$

where $E_c$ it the concrete modulus of elasticity.
The CSCT failure criterion has the following analytical expression:

$$\frac{V_{R,c}}{bd\sqrt{f_c}} = \frac{1}{6}\frac{2}{1+120\dfrac{\varepsilon d}{16+d_g}} \quad \text{[MPa,mm]} \tag{17}$$

where $V_{R,c}$ is the static shear strength, $f_c$ the concrete compressive strength measured in cylinders and $d_g$ the maximum aggregate size.

The failure load can be determined by the intersection of the shear force-strain relationship (which is related to the bending moment-strain relationship) with the failure criterion (by substituting Eq. (15) into Eq. (17)). For high-strength concrete ($f_c$>60 MPa) or light-weight concrete $d_g$ should be taken equal to zero because the critical shear crack develops through the aggregates.

The control section for three or four-point bending tests on beams is located at $d/2$ from the point load.

### A2) Shear strength according to *fib*-Model Code 2010

The shear strength ($V_{R,c}$) according to fib-Model Code 2010 is given by

$$V_{R,c} = k_v\sqrt{f_c}\,z\,b_w \quad [f_c \text{ in MPa}] \tag{18}$$

where the effective shear depth can be taken as $0.9d$ (being $d$ the effective flexural depth), $b_w$ is the member width, $f_c$ is the concrete compressive strength and $f_c^{1/2}$ shall not be taken as greater than 8MPa.

For a Level II approximation, $k_v$ is determined with:

$$k_v = \frac{0.4}{1+1500\varepsilon_x}\frac{1300}{1000+k_{dg}z} \quad [z \text{ in mm}] \tag{19}$$

Parameter $k_{dg}$ can be determined as follows:

$$k_{dg} = \frac{32}{16+d_g} \geq 0.75 \quad [d_g \text{ in mm}] \tag{20}$$

For concrete compressive strengths larger than 70 MPa and light-weight concrete $d_g$ shall be taken as zero in order to account for the loss of aggregate interlock in the cracks due to fracture of aggregates.

If no axial force is applied, the strain $\varepsilon_x$ at the mid-depth of the effective shear depth in the control section is given by:

$$\varepsilon_x = \frac{1}{2E_sA_s}\left(\frac{M_E}{z}+V_E\right) \tag{21}$$

where $E_s$ is the reinforcement modulus of elasticity, $A_s$ is the tensile reinforcement area, and $M_E$ and $V_E$ the applied bending moment and shear force, respectively.

One may determine the static shear strength by substituting Eq. (21) into Eq. (19) and then (18).

The control section for three or four-point bending tests on beams is located at $d$ from the point load.

### A3) Shear strength according to Eurocode 2

The shear strength ($V_{R,c}$ in N) according to Eurocode 2 is given by:

$$V_{R,c} = \frac{0.18}{1.0}k\left(100\rho_l f_c\right)^{1/3}b_w d \geq 0.035k^{3/2}f_c^{1/2}b_w d \tag{22}$$

where $f_c$ is the concrete compressive strength (in MPa), $b_w$ is the member width (in mm), $d$ is the effective flexural depth (in mm), $\rho_l$ is the reinforcement ratio (that shall not be taken larger than 0.02).
Parameter $k$ can be determined as:

$$k = 1+\sqrt{\frac{200}{d}} \leq 2.0 \quad [d \text{ in mm}] \tag{23}$$